Quantum dynamics of the prototype polaron model

2001 J. Phys.: Condens. Matter 13 3297

(http://iopscience.iop.org/0953-8984/13/14/306)

INSTITUTE OF PHYSICS PUBLISHING JOURNAL OF PHYSICS: CONDENSED MATTER

J. Phys.: Condens. Matter **13** (2001) 3297–3326 www.iop.org/Journals/cm PII: S0953-8984(01)18741-2

Quantum dynamics of the prototype polaron model

U Herfort and M Wagner

Institut für Theoretische Physik, Universität Stuttgart, Pfaffenwaldring 57, D-70550 Stuttgart, Germany

E-mail: herfort@theo3.physik.uni-stuttgart.de

Received 8 November 2000, in final form 6 March 2001

Abstract

The *ab initio* description of evolutionary processes in extended electron–phonon systems (polaronic transport, excitonic transfer, etc) up to the present is beyond numerical accessibility, since it requires the simultaneous knowledge of all eigenfunctions and eigenvalues. Therefore, usually rough approximations are made, such as a semiclassical treatment. However, as we have shown in a recent paper, the full quantum-mechanical treatment drastically deviates from the semiclassical approximation (even in a qualitative manner).

In the concept discussed here unitary product transformations are introduced, the constituents of which account for the two antagonistic tendencies inherent in every coupled electron–phonon Hamiltonian. We apply our procedure to the concrete case of the dimer–oscillator model by choosing for each of the antagonistic tendencies respectively a one parameter unitary operator, such that full analytical diagonalization is reached in the opposing limits of the Hamiltonian constituents. In the intermediate regime the two parameters of the transformation are suitably optimized. In this manner the generation of the full spectrum of eigensolutions involves two analytically fixed parameters only. The evolutionary behaviour resulting from our procedure is contrasted with the exact numerical result as well as with the one from the semiclassical approach and also with a more simple ('displacive') unitary transformation frequently used in the literature.

It is shown that our calculation approaches the exact result in a satisfactory manner in all intrinsic physical parameter regimes (coupling and transfer) and overcomes the drastic shortcomings of previous calculations.

1. Introduction

Although the polaron problem, after its initiation by Landau [1] in the 1930s, has already attracted long lasting research activity, it is still of great current interest. In particular new interest in polaronic concepts is in the field of superconductivity [2, 3] where Mott and his followers have advocated a Bose–Einstein condensation of bipolarons [4–6], which would lead to a Schafroth type of superconductivity [7]. Also, a growing interest is noted in

0953-8984/01/143297+30$30.00

biophysics, where e.g. models of excitonic polarons are discussed in the functional modeling of photosynthetic units [8, 9].

Another application of polaron theory is the problem of the spatial self-localization of an initially delocalized electronic excitation in crystalline systems. From the observation of retarded luminescence in rare-gas crystals [10] and in alkali halides [11] we know that a free exciton generated by optical excitation can get self-trapped at two neighbouring sites (dimerization) due to its interaction with the lattice vibrations. In this process energy is carried away from the excitonic system. This counteracts the excitonic transfer between lattice sites, which tends to delocalize the exciton.

Notwithstanding the long history of polaronic research the handling of the time evolution of polaronic exciton systems is still not at a very satisfactory stage. Computational *ab initio* calculations of realistic systems are, even today, beyond numerical accessibility.

In earlier work (e.g. references [12, 13]) on the temporal evolution of exciton(electron)–phonon systems, a procedure was usually employed which involved elements of a phenomenological nature. For example, a semiclassical approach was taken in which the phonon system was treated classically. As we have shown in a previous paper [14], this type of approximation may lead to results that not only show quantitative but even qualitative deviations from the exact solution. On the other hand, a fully quantum mechanical treatment numerically is only possible in simple cases like the two-site model (1 exciton, 1 oscillator, 2 sites).

One possibility to overcome these difficulties is to subject the coupled system to a unitary transformation which approximately diagonalizes the Hamiltonian. In this manner the temporal evolution becomes tractable in the transformed space [15, 16].

To promote the lucidity of our calculations we briefly explain the philosophy of this method. If we consider an observable A, the temporal evolution of which we desire to know after an initial state $|\Psi(0)\rangle$ has been fixed, we have to calculate the Heisenberg evolution

$$\overline{A}(t) = \langle\Psi(0)|\exp(\mathrm{i}Ht)A\exp(-\mathrm{i}Ht)|\Psi(0)\rangle \tag{1}$$

where H is the Hamiltonian of the system and where the energy unit is taken such that $\hbar = 1$. If $\{|\phi_m\rangle\}$ is the eigenbase of the Hamiltonian,

$$H|\phi_m\rangle = E_m|\phi_m\rangle. \tag{2}$$

Then there exists a unitary transformation (operator U) such that the eigenbase $\{|\phi_m\rangle\}$ may be *generated* from an *arbitrary* complete orthonormal base (CON base) $\{|\phi_m^{(0)}\rangle\}$ such that

$$|\phi_m\rangle = U|\phi_m^{(0)}\rangle \tag{3}$$

('unitary generation of the eigenbase'). This formula may be considered as the fundamental formula of our approach. The requirement that the states generated by (3) form an eigenbase of the given Hamiltonian H is equivalent to the condition that the *transformed* Hamiltonian

$$\tilde{H} = U^\dagger H U \tag{4}$$

is diagonal with respect to the given CON base $\{|\phi_m^{(0)}\rangle\}$, $U^\dagger H U|\phi_m^{(0)}\rangle = E_m|\phi_m^{(0)}\rangle$.

The basic properties of U are given by $U^\dagger U = 1$, $U^{-1} = U$ and by the conservation of the scalar product $\langle\phi \mid \psi\rangle = \langle U\phi \mid U\psi\rangle$, which includes the conservation of orthonormality, $\langle\phi_m \mid \phi_n\rangle = \delta_{mn} = \langle U\phi_m \mid U\phi_n\rangle$. For further details about unitary transformations see [17]. If we know the operator U the eigenvalue E_m is given by

$$E_m = \langle\phi_m^{(0)}|U^\dagger H U|\phi_m^{(0)}\rangle \tag{5}$$

and the projection of the initial state $|\Psi(0)\rangle$ onto the eigenbase reads

$$|\Psi(0)\rangle = \sum_m |\phi_m\rangle\langle\phi_m \mid \Psi(0)\rangle = \sum_m |U\phi_m\rangle\langle U\phi_m \mid \Psi(0)\rangle. \tag{6}$$

Then the temporal evolution of the expectation value assumes the form

$$\overline{A}(t) = \sum_{m,n} \langle \Psi(0) \mid \phi_m \rangle \langle \phi_m | \exp\bigl(\mathrm{i}(E_m - E_n)t\bigr) A |\phi_n\rangle \langle \phi_n \mid \Psi(0)\rangle \tag{7}$$

and by means of (3):

$$\overline{A}(t) = \sum_{m,n} \langle U\Psi(0) \mid \phi_m^{(0)} \rangle \langle \phi_m^{(0)} | \exp\bigl(\mathrm{i}(E_m - E_n)t\bigr) U^{\dagger} A U |\phi_n^{(0)}\rangle \langle \phi_n^{(0)} \mid U\Psi(0)\rangle. \tag{8}$$

The favourable features of this expression are as follows:

(a) One may choose a base system $\{|\phi_m^{(0)}\rangle\}$ which is easily managable, e.g. an eigenbase of some 'undisturbed' Hamiltonian H_0. (This will be done in the following.)
(b) Having made this choice, all matrix elements appearing in (7) are easily calculated, if the application of the unitary operator U onto the base vectors $|\phi_m^{(0)}\rangle$ is known, and the eigenvalues E_m appearing in (7) are also calculated in the form of a matrix element, i.e. the one given by (5).

The only quantity which remains to be fixed is the unitary operator U, which generates the eigenvectors $|\phi_m\rangle$ from $|\phi_m^{(0)}\rangle$ via the 'rotation' $U|\phi_m^{(0)}\rangle$ in Hilbert space. Naturally, in the systems we are considering it is impossible to find the exact analytic form of U. But due to the orthonormality-preserving property of any unitary operator, also simpler unitary operators may be invoked, which *simultaneously generate* a full approximate eigenbase. This is the aim of the present paper. We propose and check unitary operators, which are tailored in such a way that they incorporate the basic antagonistic tendencies of any exciton(electron)–phonon system: one tendency to localize the electron ('polaronic' effect) and another tendency which tries to delocalize the exciton (i.e. to make it freely movable). We thus will write U as a product of two operators, one for each of the two tendencies. We demonstrate this method for the example of the two-site model.

One of the two operator factors will always be taken as a 'displacement operator', which accounts for the self-trapping interaction of the electron (exciton) with the oscillatory system. This type of transformation has been frequently employed, and there is a rich literature on it. For example, we refer to the paper of Silbey and Harris [18], where a displacive type of transformation has been used to explain the tunneling breakdown in the case of Ohmic dissipation. As will be seen below this displacive operator-factor alone is not sufficient for diagonalizing the problem in the opposing limits. Rather it will be seen that sometimes this transformation leads to results which are even worse than the semiclassical one. Nevertheless, this transformation has been frequently used (see e.g. Steib *et al* [19]).

The second factor, in contrast, accounts for the delocalizing effect due to the excitonic transfer. As a second factor in the literature one has to choose an operator of 'reflective' [16] or of 'squeezing' [20] type. The choice of a 'reflective' partner will be discussed later in this work, and it turns out that it displays the unpleasant feature that there is an unphysical abrupt change of the transformational parameters in the critical transfer regime. We also will discuss shortly the 'squeezing (antisqueezing)'. This choice is the least suitable. We therefore will introduce for the partner of the displacive operator a new operator not discussed in literature so far, which we denote as an 'anticrossing' operator, and which will turn out to be overall the best choice.

In section 2 we present our model and exploit the reflective symmetry of the Hamiltonian to decouple the evolutions of the even and odd parity subspaces. In section 3 we introduce the reflective–displacive (RD) and displacive–anticrossing (DA) transformations and apply them to our model. In section 4 the semiclassical approximation is discussed. In section 5 we discuss the so-called Debye–Waller anomaly. In section 6 we present the numerical results of our

calculations and compare them with the exact and the semiclassical evolution. In section 7 we draw our conclusions. In the appendix we discuss the displacive-antisqueezing transformation as an alternative to the RD and the DA transformation.

2. The model

2.1. Hamiltonian of the system and initial condition

We consider the standard symmetric dimer consisting of two excitonic (electronic) sites, coupled to a single harmonic oscillator [14]. The Hamiltonian reads ($\hbar = 1$)

$$H = \tfrac{1}{2}(P^2 + Q^2 - 1) - T\,(|l\rangle\langle r| + |r\rangle\langle l|) + DQ\,(|l\rangle\langle l| - |r\rangle\langle r|) \tag{9}$$

where $|l\rangle$ and $|r\rangle$ are the site states of the exciton, and the frequency of the oscillator has been chosen as the energy measure of the system, i.e., it is taken as unity. The zero point energy has been subtracted from H. To assert inversion symmetry we require $|r\rangle$ to be the mirror image of $|l\rangle$ and Q to be an odd coordinate such that $R_Q Q = -QR_Q$ (R_Q: reflection operator in Q-subspace). Without loss of generality we assume T to be positive. As an initial condition we assume that at time $t = 0$ an exciton is created in the left-site state, keeping the oscillator in its unperturbed ground state $|\phi_0^{(0)}\rangle$:

$$|\Psi(t=0)\rangle = |l\rangle|\phi_0^{(0)}\rangle. \tag{10}$$

The aim of this paper is to determine the temporal evolution of the excitonic occupation probability difference

$$z(t) = \langle\Psi(t)|\,(|l\rangle\langle l| - |r\rangle\langle r|)\,|\Psi(t)\rangle \tag{11}$$

for this initial condition.

2.2. The Fulton–Gouterman transcription

Since the Hamiltonian (9) is invariant with respect to inversion of the total (exciton + oscillator) system, the eigenstates must display a definite parity $p = \pm 1$, i.e., they must be of the general Wigner form

$$|\psi_n^{(p)}\rangle = \frac{1}{\sqrt{2}}\left(|l\rangle + p|r\rangle R_Q\right)|\phi_n^{(p)}\rangle \tag{12}$$

where $|r\rangle$ is assumed to be the mirror image of $|l\rangle$, R_Q is the inversion operator of the oscillatory system, and $|\phi_n^{(p)}\rangle$ are states in the subspace of the oscillator. The oscillatory 'companion functions' $|\phi_n^{(p)}\rangle$ must obey the Fulton–Gouterman (FG) equations [20–24]

$$H_{\mathrm{FG}}^{(p)}|\phi_n^{(p)}\rangle := \left(\tfrac{1}{2}(P^2 + Q^2 - 1) - pTR_Q + DQ\right)|\phi_n^{(p)}\rangle = E_n^{(p)}|\phi_n^{(p)}\rangle. \tag{13}$$

Each FG Hamiltonian $H_{\mathrm{FG}}^{(p)}$, $p = \pm 1$, operates only in one of the two parity subspaces, whence the temporal evolutions in the two subspaces are completely decoupled:

$$|\Psi(t)\rangle = \frac{1}{\sqrt{2}}\sum_p \left(|l\rangle + p|r\rangle R_Q\right)|\Phi^{(p)}(t)\rangle \tag{14}$$

where

$$\begin{aligned}|\Phi^{(p)}(t)\rangle &= \frac{1}{\sqrt{2}}\left(\langle l| + p\langle r|R_Q\right)|\Psi(t)\rangle \\ &= \exp(-\mathrm{i}H_{\mathrm{FG}}^{(p)}t)|\Phi^{(p)}(0)\rangle = \sum_n c_n^{(p)}|\phi_n^{(p)}\rangle\exp(-\mathrm{i}E_n^{(p)}t)\end{aligned} \tag{15}$$

$$c_n^{(p)} = \langle\phi_n^{(p)} \mid \Phi^{(p)}(0)\rangle. \tag{16}$$

Our initial state (10) then corresponds to the state

$$|\Phi^{(p)}(0)\rangle = \frac{1}{\sqrt{2}}|\phi_0^{(0)}\rangle \tag{17}$$

for $p = \pm 1$.

Under these premises we now have to transcribe the expectation value (11) for the occupational probability difference. Inserting (14)–(17) in (11) we find

$$z(t) = \sum_{m,n} \langle \phi_0^{(0)} \mid \phi_m^{(+)} \rangle \langle \phi_m^{(+)} \mid \phi_n^{(-)} \rangle \langle \phi_n^{(-)} \mid \phi_0^{(0)} \rangle \cos\big((E_m^{(+)} - E_n^{(-)})t\big) \tag{18}$$

which is the concretization of formula (7) to our problem.

2.3. The specification of the unitary transformation concept to our model

We now apply the concept of a unitary generation of the eigenstates to the Fulton–Gouterman equations (13); we generate its eigenfunctions $|\phi_n^{(p)}\rangle$, $p = \pm 1$, for each parity separately, as described in section 1,

$$|\phi_n^{(p)}\rangle = U_{(p)}|\phi_n^{(0)}\rangle \qquad p = \pm 1 \tag{19}$$

where $\{|\phi_n^{(0)}\rangle\}$ now is the eigenbase of the undisturbed harmonic oscillator. Expression (18) then assumes the form

$$z(t) = \sum_{m,n} \langle \phi_0^{(0)}|U_{(+)}|\phi_m^{(0)}\rangle \langle \phi_m^{(0)}|U_{(+)}^{\dagger}U_{(-)}|\phi_n^{(0)}\rangle \langle \phi_n^{(0)}|U_{(-)}^{\dagger}|\phi_0^{(0)}\rangle \cos\big((E_m^{(+)} - E_n^{(-)})t\big) \tag{20}$$

where

$$E_m^{(p)} = \langle \phi_m^{(p)}|H_{\mathrm{FG}}^{(p)}|\phi_m^{(p)}\rangle = \langle \phi_m^{(0)}|U_{(p)}^{\dagger}H_{\mathrm{FG}}^{(p)}U_{(p)}|\phi_m^{(0)}\rangle. \tag{21}$$

We emphasize that both $H_{\mathrm{FG}}^{(p)}$ and the unitary operators $U_{(p)}$ to be introduced are acting (due to the FG transformation) in the oscillator subspace. But naturally, all formulae retrospectively may be written in original product Hilbert space. Thus, the unitary operator $\hat{U}$ in the original space must be taken as

$$\hat{U} = \hat{U}_{(+)}\hat{U}_{(-)} \tag{22}$$

where

$$\hat{U}_{(p)} = \frac{1}{\sqrt{2}}(|l\rangle + p|r\rangle R_Q)U_{(p)}\frac{1}{\sqrt{2}}(\langle l| + p\langle r|R_Q). \tag{23}$$

For the calculation this return to the original space is not needed (see expression (20)).

3. Unitary product transformations

3.1. RD transformation

3.1.1. Definition In previous work [20], it has been shown that there exists a specific product transformation which has the quality of reproducing the ground state properties over the full combination range of the basic parameters D (coupling) and T (transfer). Recently [25] it has been shown that this transformation is not only adequate for the ground state, but that it also yields the analytically correct behaviour for the full eigenvalue spectrum in the two opposite limiting cases

(i) $D \to 0$, T arbitrary,
(ii) D arbitrary, $T \to 0$,

which is tantamount to a full diagonalization of the Hamiltonian in these limits. Adopting respectively the limiting analytic forms of the parameters inherent in the transformation operators and comparing the approximate eigenvalues with the numerically exact ones it is found that also in intermediate parameter ranges the approximation remains remarkably good.

The transformation considered is of the form

$$U_{rd} = U_r(\beta)U_d(\delta) \tag{24}$$

where β and δ, which are taken as real quantities, constitute the parameters of the transformation. The first of the two transformations, U_r, is given by

$$U_r(\beta) = \mathrm{e}^{S_r} = \cos(\beta Q) + \sin(\beta Q)R_Q \tag{25}$$

$$S_r = -S_r^\dagger = \beta Q R_Q. \tag{26}$$

It is of reflective nature and has the properties

$$T_r : Q = U_r^\dagger Q U_r = \cos(2\beta Q)Q + \sin(2\beta Q)QR_Q \tag{27}$$

$$T_r : P = U_r^\dagger P U_r = \cos(2\beta Q)P + \sin(2\beta Q)PR_Q + \mathrm{i}\beta\sin(2\beta Q) - \mathrm{i}\beta\cos(2\beta Q)R_Q \tag{28}$$

$$T_r : R_Q = U_r^\dagger R_Q U_r = \cos(2\beta Q)R_Q - \sin(2\beta Q) \tag{29}$$

$$U_r|\phi(Q)\rangle = \cos(\beta Q)|\phi(Q)\rangle + \sin(\beta Q)|\phi(-Q)\rangle. \tag{30}$$

This transformation supplements an oscillatory wavefunction by a diminished mirror image of itself (see figure 1).

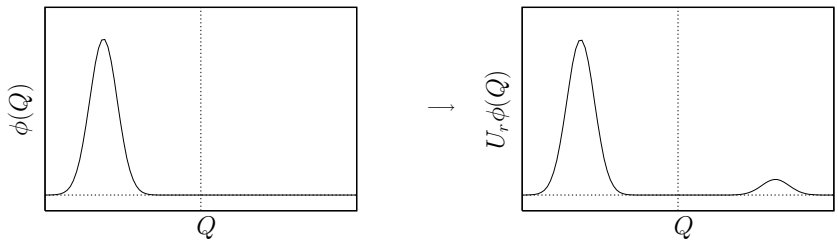

Figure 1. The reflective transformation U_r.

The second transformation, U_d, is given by

$$U_d(\delta) = \mathrm{e}^{S_d} \tag{31}$$

$$S_d = -S_d^\dagger = \mathrm{i}\delta P. \tag{32}$$

It is of displacive type and has the properties

$$T_d : Q = U_d^\dagger Q U_d = Q - \delta \tag{33}$$

$$T_d : P = U_d^\dagger P U_d = P \tag{34}$$

$$T_d : R_Q = U_d^\dagger R_Q U_d = \mathrm{e}^{-2\mathrm{i}\delta P}R_Q \tag{35}$$

$$U_d|\phi(Q)\rangle = |\phi(Q+\delta)\rangle. \tag{36}$$

This transformation displaces the oscillatory wavefunction from its original position (see figure 2).

We note that this transformation has been frequently used in literature and is known as the 'Lang–Firsov' transformation. The special form $U_d(\delta = D)$ of this transformation, i.e. the one choosing for the displacement parameter δ the fixed, non-optimized value $\delta = D$, has been used in the work of Steib *et al* [19]. We will denote this specific transformation as the 'simple

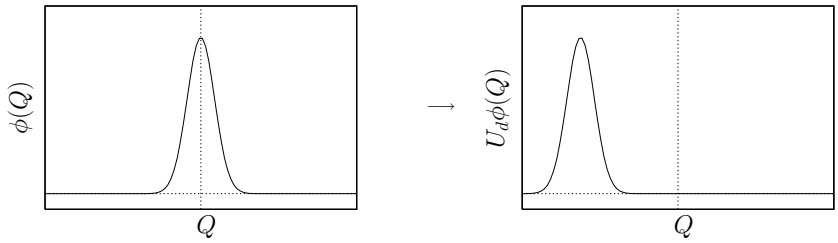

Figure 2. The displacive transformation U_d.

displacement transformation D' and contrast the results pertaining to this transformation with those derived from our product transformations RD and DA (see later).

It should be noted that the RD transformation (24) is equivalent to the Fröhlich transformation for small values of β and δ, but has the advantage that it can be written down in closed form [24].

The transformed Hamiltonian reads

$$\begin{aligned}\tilde{H}_{\mathrm{FG}}^{(p)} = T : H_{\mathrm{FG}}^{(p)} &= U^{\dagger} H_{\mathrm{FG}}^{(p)} U \\ &= \tfrac{1}{2}[(Q-\delta)^2 + P^2 - 1 - 2\mathrm{i}\beta P \mathrm{e}^{-2\mathrm{i}\delta P} R_Q + \beta^2] \\ &\quad + D\cos\bigl(2\beta(Q-\delta)\bigr)(Q-\delta) + D\sin\bigl(2\beta(Q-\delta)\bigr)(Q-\delta)\mathrm{e}^{-2\mathrm{i}\delta P} R_Q \\ &\quad - pT\cos\bigl(2\beta(Q-\delta)\bigr)\mathrm{e}^{-2\mathrm{i}\delta P} R_Q + pT\sin\bigl(2\beta(Q-\delta)\bigr). \end{aligned} \tag{37}$$

3.1.2. Contrast to squeezing-type transformations We mention that in the literature another product transformation has sometimes has used to treat our archetype model, which applied to the original Hamiltonian (9) is a product of a special Lang–Firsov transformation and an antisqueezing transformation in the exciton–phonon space. If we translate this transformation into the FG picture it amounts to a product of a displacive and an antisqueezing operator. We will contrast it with the one chosen by us and show that it only achieves diagonalization in the weak-coupling limit and also only for the ground state of the system (see appendix).

3.1.3. The small-coupling and the large-transfer cases For $D = 0$ the Hamiltonian is diagonal, since the eigenfunctions of $P^2 + Q^2$ are also those of R_Q. When we expand $\tilde{H}_{\mathrm{FG}}^{(p)}$ up to the linear terms in D, β, δ, we obtain

$$\begin{aligned}\tilde{H}_{\mathrm{FG}}^{(p)} = \tfrac{1}{2}(P^2 + Q^2 - 1) + (D - \delta + 2pT\beta)\, Q + \mathrm{i}\,(2\delta pT - \beta)\, P R_Q - pT R_Q \\ + O(\delta^2, \beta^2, \beta\delta, \delta D, \beta D) + O(\delta^2, \beta^2)T. \end{aligned} \tag{38}$$

The linear terms vanish if

$$\delta = \frac{D}{1-4T^2} \qquad \beta = \frac{2pTD}{1-4T^2} \tag{39}$$

which amounts to the Fröhlich condition

$$[H_1, S_d + S_r] = -W_1 \tag{40}$$

where

$$H_1 = \tfrac{1}{2}(P^2 + Q^2 - 1) - pT R_Q \tag{41}$$

$$W_1 = DQ. \tag{42}$$

The diagonal part of $\tilde{H}_{\mathrm{FG}}^{(p)}$ is then correct up to second order inclusive and the energy calculation corresponds to second-order perturbation theory:

$$E_m^{(p)} = m - (-1)^m pT + \left((-1)^m(2m+1)pT - \tfrac{1}{2}\right)\frac{D^2}{1-4T^2} + O(D^3) \qquad (43)$$

which is correct to order D^2 inclusively. This diagonalization holds in the limiting case of small transfer ($D \ll 1$) for all states (not only the ground state) and for all values of T except near the point $T = \frac{1}{2}$ where the free exciton is in resonance with the oscillator. In the small-coupling regime the RD transformation is therefore equivalent to second-order standard perturbation theory. In particular it is worth noting that the exact perturbative small coupling limit, which corresponds to the Fröhlich condition (40) and to the results (39) cannot be established by a displacive transformation alone, since the latter would require $\beta = 0$ in contradiction to result (39).

From (37) we observe that for large transfer ($T \gg 1$) the condition $D \ll 1$ for the validity of the parameter choice (39) may be relaxed to $D^2 \ll T$. In this case, the transformation parameters take the approximate values

$$\delta = -\frac{D}{4T^2} \qquad \beta = -\frac{D}{2pT} \qquad (44)$$

and the energy eigenvalues, up to order D^2/T inclusively, read

$$E_m^{(p)} = m - (-1)^m pT - \frac{(-1)^m(m+\frac{1}{2})D^2}{2pT} + [1-(4m+2)D]\frac{D^2}{8T^2} + O\left(D\left(\frac{D}{T}\right)^3\right). \qquad (45)$$

3.1.4. The small-transfer case (coupling D arbitrary) The small transfer case ($T \ll 1$) was considered by one of us in reference [26]. The method employed there is equivalent to setting $\delta = D$ and varying only β. In this case the ground state energy is minimized for

$$\delta = D \qquad \beta = \frac{2pTD}{4D^4 + 6D^2 + 1} \qquad (46)$$

and in the two limiting cases $D \ll 1$ and $D \gg 1$ this parameter choice also strongly reduces the non-diagonality of the Hamiltonian. The analytically exact second order result in this limit ($T \ll 1$) was found in a perturbative manner in reference [26] and in an alternative way by Rapp [25]. For the ground state it is of the form

$$E_0^{(p)} = -\tfrac{1}{2}D^2 - \mathrm{e}^{-D^2}pT - \mathrm{e}^{-2D^2}[E\mathrm{i}(2D^2) - \gamma - \log(2D^2)]T^2 + O(T^3), \qquad (47)$$

where $\gamma = 0.577215\ldots$ denotes Euler's constant (see reference [27], p xxx) and

$$E\mathrm{i}(z) = \gamma + \log z + \sum_{n=1}^{\infty}\frac{z^n}{n\,n!} \qquad (48)$$

is the exponential-integral function (see reference [27], p 935). For elevated states the perturbation results may be found in a similar manner.

We now intend to show that our unitary transformation has the capacity to reproduce the analytical result in both the small ($D \ll 1$) and large ($D \gg 1$) coupling regime, if the parameters δ, β are chosen in the form (46).

We first consider the case $D \ll 1$, such that now both $D \ll 1$ and $T \ll 1$. Then $\beta = 2pTD + O(T^3)$, which agrees with (39). The perturbative ground state energy (47) in this limit ($T \ll 1$, $D \ll 1$) agrees with (43) up to second order in D and T inclusive.

In the strong coupling limit ($D \gg 1$), diagonalization of all states up to order T^2/D^2 is obtained for $\beta = \frac{1}{2}pT/D^3$. The expression for the ground state eigenvalue reads

$$E_0^{(p)} = \tfrac{1}{2} - \tfrac{1}{2}D^2 - \mathrm{e}^{-D^2}pT - \frac{T^2}{2D^2} + O(T^2/D^4, T^3). \qquad (49)$$

This result coincides with (47) up to second order in D^{-1} and T, as can be seen using the asymptotic representation

$$Ei(z) = \frac{e^z}{z}[1 + O(z^{-1})]. \tag{50}$$

3.1.5. The general case (D, T arbitrary) In the general case we calculate the expectation value of $\tilde{H}_{\mathrm{FG}}^{(p)}$ for the eigenstates $|\phi_m^{(0)}\rangle$ of the unperturbed oscillator as a function of β and δ:

$$\begin{aligned} E_m^{(p)}(\beta,\delta) = \langle m|\tilde{H}_{\mathrm{FG}}^{(p)}|m\rangle = m + \tfrac{1}{2}(\beta^2+\delta^2) \\ -(-1)^m\beta\delta\exp(-\delta^2)\big[L_m^{(1)}(2\delta^2) + L_{m-1}^{(1)}(2\delta^2)\big] \\ +D\beta\exp(-\beta^2)\sin(2\beta\delta)\big[L_m^{(1)}(2\beta^2) + L_{m-1}^{(1)}(2\beta^2)\big] \\ -D\delta\exp(-\beta^2)\cos(2\beta\delta)L_m^{(0)}(2\beta^2) \\ -pT\exp(-\beta^2)\sin(2\beta\delta)L_m^{(0)}(2\beta^2) \\ -(-1)^m pT\exp\big(-(\beta^2+\delta^2)\big)L_m^{(0)}\big(2(\beta^2+\delta^2)\big) \\ +(-1)^m D\beta\exp\big(-(\beta^2+\delta^2)\big)\big[L_m^{(1)}\big(2(\beta^2+\delta^2)\big) \\ +L_{m-1}^{(1)}\big(2(\beta^2+\delta^2)\big)\big] \end{aligned} \tag{51}$$

where $L_m^{(k)}$ denote the generalized Laguerre polynomials. In principle the transformational parameters β and δ could be determined by numerical optimization. But since we desire to fix δ and β uniquely in such a way that they are the same for all eigenstates, we adopt a different approach. We consider the two analytical expressions (39) and (46), which are valid in the limiting cases $T \to \infty$ and $T \to 0$ respectively, and choose the former for all T above a critical value T_c, and the latter for T below T_c. For a given value of D we define the accurate position of T_c as that of T where both parameters switch their sign if in each of the parity cases the lowest state is minimized. For small D values ($D < \frac{1}{2}$) it is given by $T_c \approx \frac{1}{2}$, and for higher D values ($D > 1$) it increases ($D = 0.5$: $T_c \approx 0.7$; $D = 1$: $T_c \approx 1.0$; $D = 2$: $T_c \approx 2.7$; $D = 4$: $T_c \approx 8$). For calculational purposes the abruptness of the sign switches at T_c has been smoothed somewhat by using the following interpolating expressions for β and δ:

$$\begin{aligned} \beta = pTD\Bigg\{\frac{1-4T^2}{\epsilon^2+(1-4T^2)^2}\big[1+\tanh\big(\gamma(T-T_c)\big)\big] \\ +\frac{1}{4D^4+6D^2+1}\big[1-\tanh\big(\gamma(T-T_c)\big)\big]\Bigg\} \end{aligned} \tag{52}$$

$$\delta = \frac{D}{2}\Bigg\{\frac{1-4T^2}{\epsilon^2+(1-4T^2)^2}\big[1+\tanh\big(\gamma(T-T_c)\big)\big] + \big[1-\tanh\big(\gamma(T-T_c)\big)\big]\Bigg\} \tag{53}$$

$$\gamma = \frac{20}{D} \qquad \epsilon = 0.1 \qquad T_c = \tfrac{1}{2}(D^2+1). \tag{54}$$

Figure 3 demonstrates the accuracy of the eigenvalues generated via our unitary product transformation for $D = 0.25$ as a function of T, as compared with the numerically exact curves. We note the discrepancies in the critical T regime around $T_c \approx 0.5$; however, at some appropriate distance from T_c above and below T_c the approximate eigenvalues smoothly approach the exact ones simultaneously for all quantum numbers. We find a similar situation for other D-values. We refrain therefore from illustrating the behaviour in other cases.

After the transformational parameter values $\beta^{(p)}, \delta^{(p)}$ have been obtained for each parity in the way described above, we have to insert the operator $U_{rd}(\beta^{(\pm)}, \delta^{(\pm)}) = U_r(\beta^{(\pm)})U_d(\delta^{(\pm)})$ in expression (20), which allows us to calculate the time evolution of the occupational probability

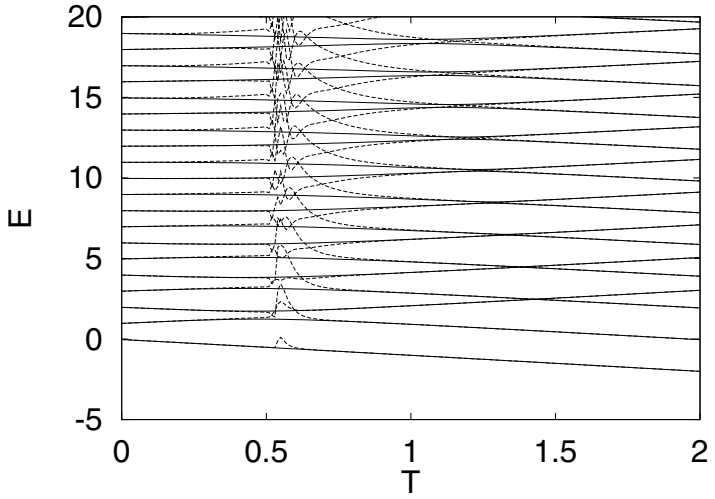

Figure 3. Comparison of the eigenvalues generated via our RD transformation as a function of T with the numerically exact curves for $D = 0.25$ and $p = +1$. Solid lines: exact numerical diagonalization, dashed lines: RD result.

difference. (In place of the parity characterization $U_\pm$ we denote it via superscripts at the parameters $\beta^{(\pm)}$, $\delta^{(\pm)}$.)

The results of these calculations are presented in section 6.

3.2. The DA transformation

3.2.1. Motivation In the previous section it was shown that the RD transformation in the small coupling regime is able to diagonalize the Hamiltonian H_{FG} with high accuracy, except for a small range of the transfer parameter T near the critical value T_c. The reason for this failure near T_c can be seen from the behaviour of the exact eigenenergies for $D = 0$: At $T = 0.5$ the energies of neighbouring states with even and odd oscillatory quantum number n become equal. If now a small coupling D is switched on, the degeneracy is removed. These avoided crossings are clearly visible from the solid lines in figure 3, which show the dependency of the energy eigenvalues as functions of the transfer T for $D = 0.5$. For this reason the mutual correspondence between the oscillatory states $|n\rangle := |\phi_n^{(0)}\rangle$ and the approximate eigenstates $|\phi_n^{(p)}\rangle$ of H_{FG} is different in the two limiting cases $T \to 0$ and $T \to \infty$. For example, in the odd parity subspace $p = -1$, for $T \to 0$ the oscillatory state $|1\rangle$ is mapped by U_{rd} onto the first excited state $|\phi_1^{(-1)}\rangle$ of H_{FG}, for $T \to \infty$ onto the ground state $|\phi_0^{(-1)}\rangle$. If T increases continually from 0 to ∞, the mutual correspondence has to change abruptly at some value of T. This is the reason for the jump of the transformation parameters β and δ at the critical transfer T_c. Since in our RD transformation the parameters $\beta^{(p)}$ and $\delta^{(p)}$ both have been taken as smooth functions of T in the critical region, the energy values from our transformation must cross the gap between the exact values and therefore cannot reproduce the exact values.

In order to overcome this shortcoming, we need a transformation U_a with the following properties:

- For $T \to 0$, U_a approaches the identity transformation.
- For $T \to \infty$, U_a exchanges neighbouring states with each other, namely $|1\rangle$ with $|2\rangle$, $|3\rangle$

with $|4\rangle$, etc for even parity, and $|0\rangle$ with $|1\rangle$, $|2\rangle$ with $|3\rangle$, etc for odd parity.

A transformation fulfilling these two conditions will be called an anticrossing transformation in this paper. In figure 4 the energetic effect of an anticrossing transformation is vizualized.

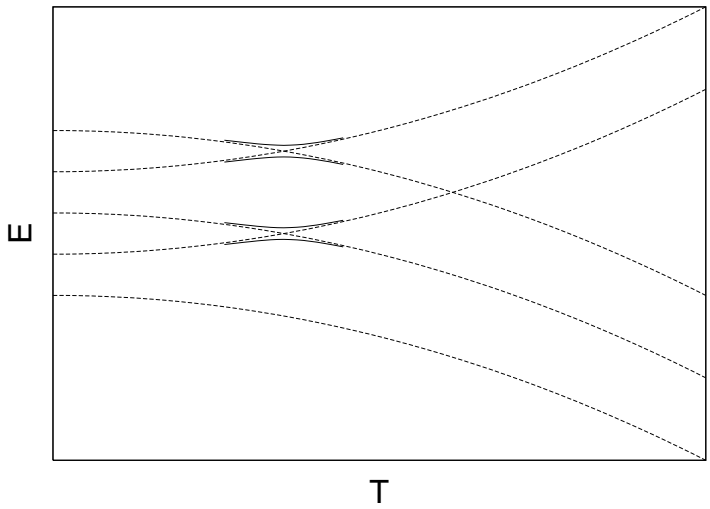

Figure 4. Illustration of the energetic effect of an anticrossing transformation.

3.2.2. Definition According to our concept (given in the introduction) we want to have approximately

$$|\phi_n^{(p)}\rangle \equiv U_{da}|\phi_n^{(0)}\rangle \equiv U_d(\delta)U_a(\alpha)|\phi_n^{(0)}\rangle \tag{55}$$

where the anticrossing operator is taken as

$$U_a(\alpha) = \exp S_a(\alpha) \qquad S_a(\alpha) = b(1 + pR_Q)\alpha(b^\dagger b) - \alpha(b^\dagger b)(1 + pR_Q)b^\dagger \tag{56}$$

and $\alpha(x)$ is a real-valued function of one variable. Application of U_a to the oscillatory states yields

- for even parity:

$$S_a|2n\rangle = \lambda_n|2n-1\rangle \tag{57}$$
$$S_a|2n-1\rangle = -\lambda_n|2n\rangle \tag{58}$$
$$U_a|2n\rangle = \cos\lambda_n|2n\rangle + \sin\lambda_n|2n-1\rangle \tag{59}$$
$$U_a|2n-1\rangle = \cos\lambda_n|2n-1\rangle - \sin\lambda_n|2n\rangle \tag{60}$$

  where $\lambda_n = 2\alpha(2n)\sqrt{2n}$;
- for odd parity:

$$S_a|2n\rangle = -\lambda_n|2n+1\rangle \tag{61}$$
$$S_a|2n+1\rangle = \lambda_n|2n\rangle \tag{62}$$
$$U_a|2n\rangle = \cos\lambda_n|2n\rangle - \sin\lambda_n|2n+1\rangle \tag{63}$$
$$U_a|2n+1\rangle = \cos\lambda_n|2n+1\rangle + \sin\lambda_n|2n\rangle \tag{64}$$

  where $\lambda_n = 2\alpha(2n+1)\sqrt{2n+1}$;

i.e., U_a gives a rotation in the subspaces spanned by two neighbouring oscillatory states, as required above for an anticrossing transformation. This is illustrated in figure 4 for states $|1\rangle$ and $|2\rangle$ in the case of odd parity.

From equations (57) to (64) it is obvious that only the values of $\alpha(x)$ at $x = 2n$ (for even parity) or at $x = 2n + 1$ (for odd parity) are relevant. These function values, or alternatively the rotation angles λ_n, are free parameters which can be chosen in a way that diagonalizes the Hamiltonian as much as possible. This is done by requiring that the non-diagonal matrix elements of the transformed Hamiltonian $\tilde{H}_{\mathrm{FG}}^{(p)} = U_{da}^{\dagger} H_{\mathrm{FG}}^{(p)} U_{da}$ between two neighbouring states vanish, i.e. that we have for even parity

$$\langle 2n-1|\tilde{H}_{\mathrm{FG}}^{(+1)}|2n\rangle = 0 \tag{65}$$

and for odd parity

$$\langle 2n+1|\tilde{H}_{\mathrm{FG}}^{(-1)}|2n\rangle = 0. \tag{66}$$

3.2.3. The small-coupling and the large-transfer cases When in (56) α is chosen independent of n and the creation and annihilation operators $b^{\dagger}$ and b are expressed in terms of the position and momentum operators Q and P, we obtain

$$S_a(\alpha) = \mathrm{i}\sqrt{2}\alpha P + \sqrt{2}\alpha p Q R_Q \tag{67}$$

and

$$S_d(\delta) + S_a(\alpha) = \delta + \sqrt{2}\alpha)P + \sqrt{2}\alpha p Q R_Q. \tag{68}$$

Since the latter expression has the same form as $S_r + S_d$ in the case of the RD transformation (linear in P and Q), the Fröhlich condition (40) is fulfilled by the DA transformation for the parameter choice

$$\delta_{da} = \frac{D}{1+2T} \qquad \alpha_{da} = \frac{\sqrt{2}T D}{1-4T^2}. \tag{69}$$

Therefore the DA transformation, like the RD transformation, diagonalizes the Hamiltonian in the limiting cases of small coupling or large transfer and is equivalent to second-order perturbation theory.

3.2.4. The small-transfer case In the case of vanishing transfer ($T = 0$) the system is diagonalized exactly for $\delta = D$ and $\alpha_n = 0$, i.e., the DA transformation reduces to a simple displacive transformation. For small but finite values of T we have no analytical results, but the exact diagonalization for $T = 0$ means that for $T \to 0$ the approximated eigenstates and energies must approach the exact ones. Also, for large values of the coupling D the effective strength of the transfer is reduced, so that the system is even closer to the exactly solvable case $T = 0$; whereas for small values of D the Fröhlich condition can be fulfilled, as shown above. Therefore in both cases the DA transformation can be expected to yield good approximations for the energy eigenstates and eigenvalues.

3.2.5. The general case In the general case we face the problem of finding values for the transformational parameters δ and $\alpha(n)$ which yield a good approximation for all eigenstates of the Hamiltonian. In the case of the RD transformation this aim was reached by interpolating between the analytical expressions for the small and large transfer cases. For the DA transformation we have no analytical result in the small transfer case. On the other hand, for given parity p and any fixed value of δ the optimal values of the anticrossing parameters $\alpha(n)$ are uniquely determined by equations (65) and (66) for even or odd parity, respectively, separately

for each pair of neighbouring states. Only the displacive parameter δ has to be chosen the same for all states. In the present paper this is done by minimizing the ground state energy of the transformed Hamiltonian. In contrast to the case of the RD transformation, this results in a smooth dependency of δ on the system parameters T and D for each parity p.

The parameter values obtained in this way are then used to calculate the temporal evolution by inserting the operators $U_{da}(\alpha^{(\pm)}, \delta^{(\pm)})$ in (20), analogous to the RD transformation.

Figure 5 shows the T-dependence of the DA approximation of the eigenvalues for $D = 0.25$ and demonstrates the efficiency of the transformation as well as the improvement beyond the RD approximation (see figure 3). Further figures of the RD and DA results are given later.

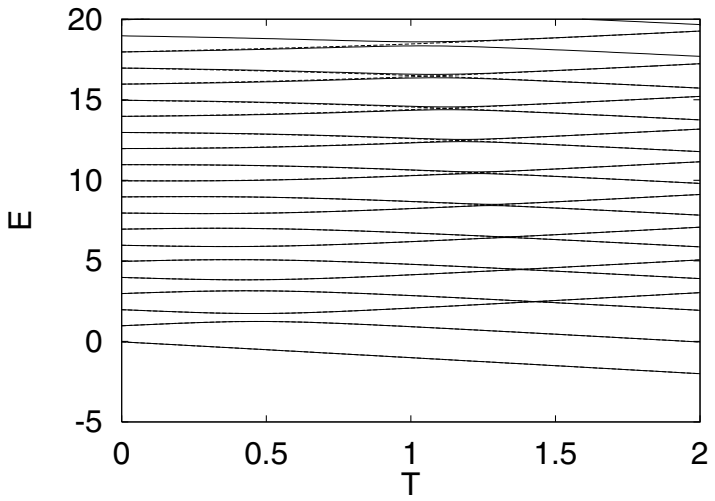

Figure 5. Comparison of the eigenvalues generated via our DA transformation as a function of T with the numerically exact curves for $D = 0.25$ and $p = +1$. Solid lines: exact numerical diagonalization, dashed lines: DA result (almost identical to exact result).

4. The semiclassical approximation

Since we intend to contrast our present results with those of the semiclassical approximation, we briefly review that now. The semiclassical approximation has been considered by Holstein [21], by Kenkre and Campbell [28], and by Esser and Schanz [13] and has been contrasted to the exact numerical solution in our earlier paper [14]. It is obtained by requiring a product form of the wave function at all times:

$$|\Psi(t)\rangle \equiv \mathrm{e}^{-\mathrm{i}Ht}|\Psi(0)\rangle \approx |\Phi_{\mathrm{exc}}(t)\rangle|\Phi_{\mathrm{osc}}(t)\rangle \tag{70}$$

where

$$|\Phi_{\mathrm{exc}}(t)\rangle = g_l(t)|l\rangle + g_r(t)|r\rangle \qquad |g_l|^2 + |g_r|^2 = 1. \tag{71}$$

We introduce the three Bloch operators

$$\hat{x}(t) = \big[|l\rangle\langle r| + |r\rangle\langle l|\big]_t \tag{72}$$

$$\hat{y}(t) = \mathrm{i}\big[|r\rangle\langle l| - |l\rangle\langle r|\big]_t \tag{73}$$

$$\hat{z}(t) = \big[|l\rangle\langle l| - |r\rangle\langle r|\big]_t. \tag{74}$$

The Heisenberg equations of motion for the momentum operator $\hat{P}$, the position operator $\hat{Q}$, and the three Bloch operators may be simplified, if the expectation values of products of operators are replaced by the products of the expectation values. Then a closed systems of differential equations is obtained for the expectation values of $\hat{P}$, $\hat{Q}$, $\hat{x}$, $\hat{y}$, and $\hat{z}$:

$$\dot{x} = -2DQy \tag{75}$$

$$\dot{y} = 2(Tz + DQx) \tag{76}$$

$$\dot{z} = -2Ty \tag{77}$$

$$\dot{Q} = P \tag{78}$$

$$\dot{P} = -(Q + Dz). \tag{79}$$

We do not go into details of this approach, but refer to an overview given in our previous paper [14].

A remarkable feature of the semiclassical model is the contrast between the symmetry breaking of the ground state, which occurs for $D^2/T > 1$ (see [13]) and the self-trapping of the temporal evolution, which occurs only for $D^2/T > 2$ in the small transfer limit (see [28]).

5. Debye–Waller peculiarity

In the expansion of the energy eigenvalues with respect to the transfer parameter T a remarkable peculiarity was found in reference [26]: The Debye–Waller screening factor $\exp(-D^2)$ is absent in all terms of even power in T. This constitutes a rigorous analytic result. Since the even power terms in T are independent of the parity p (see (47)), the energy differences between corresponding states of different parity and the same quantum number are not affected by the Debye–Waller peculiarity. These results are discussed in further detail by Firsov *et al* in [29] and [30].

In this context a glance at other types of unitary transformations is fruitful. In particular we consider a specific alternative product transformation, which has been used in the literature. This transformation also involves a product of unitary operators, but in place of our reflective factor an *antisqueezing type* of unitary factor is employed. In the appendix it is shown that this 'displacive-antisqueezing' transformation fails to reproduce the Debye–Waller peculiarity. It shows a Debye–Waller screening factor in all powers of T.

6. Numerical results

In our present study the motivation for choosing the two-site model has been the possibility of calculating the exact numerical solution, which may thus serve as a benchmark for the unitary transformation method introduced here. For the exact numerical eigensolution the FG Hamiltonian (13) is taken in its matrix representation with respect to the unperturbed eigenstates $|\phi_n^{(0)}\rangle$ of the oscillator, and this matrix subsequently is diagonalized numerically. Since the number of oscillatory states is infinite, only the first N of them were used, where N was chosen so large that the results are not changed by a further increase of N. The temporal evolution of the system then is calculated by projecting the initial state onto the numerically obtained eigenstates of $H_{\mathrm{FG}}^{(p)}$ (see (20)).

In order to judge the quality of the approximate diagonalization obtained by our RD and DA transformations, in this section the exact numerical results for the energy eigenvalues are contrasted with

(a) the results of the RD ansatz (section 3.1)

(b) the results of the DA ansatz (section 3.2)
(c) the results of a simple displacive ansatz, as it is used by Steib *et al* [19]

as functions of the coupling D for two values of the transfer T.

For the temporal evolution of the occupational probability difference quantity $z(t)$ (definition see expression (11)) we respectively choose a large and a small value of the Hamiltonian parameters D and T and provide the combinations small–small, large–large, small–large and large–small. We contrast the exact numerical results to

(a) the results of the RD ansatz (section 3.1)
(b) the results of the DA ansatz (section 3.2)
(c) the results of the semiclassical approximation (section 4)
(d) the results of the simple displacive ansatz [19].

To save space, only the most instructive of the above mentioned approximations are shown for each parameter combination.

6.1. Small transfer regime

6.1.1. Energy curves In the small transfer regime ($T = 0.25$) the simple displacive transformation (see e.g. Steib *et al* [19]) with the displacement parameter fixed at $\delta = D$ yields almost quantitatively correct values of the eigenenergies both for the low-lying levels ($n < 15$, see figure 6) and for high levels ($n \approx 100$, figure 7). This was to be expected because for $T = 0$ the displacive transformation exactly diagonalizes the Hamiltonian, as mentioned in section 3.2.

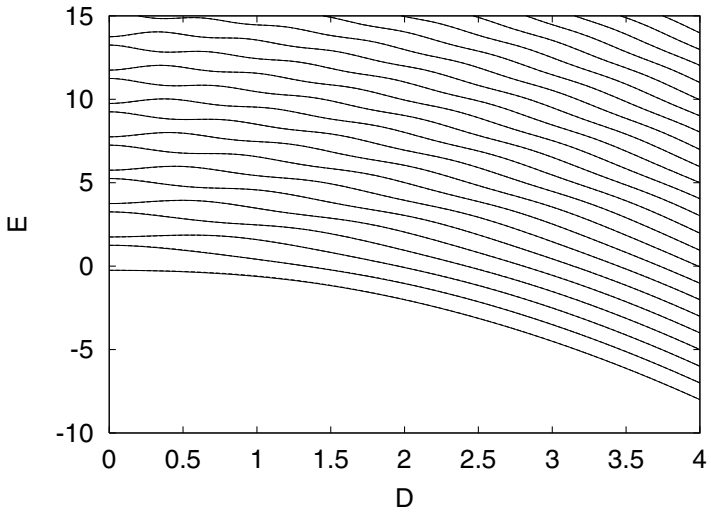

Figure 6. Comparison of the eigenvalues generated via the purely displacive transformation as a function of D with the numerically exact curves for $T = 0.25$ and $p = +1$. The two results are indiscernible on the scale of this figure.

The DA results show slight deviations from the exact values for small n (figure 8). For high n the deviations are larger (these are not shown here). At first this seems surprising since the DA transformation contains the displacive one as a special case. But it should be remembered from section 3.2 that the displacement parameter δ for the DA transformation was obtained by minimizing the ground state energy, which does not necessarily lead to a value

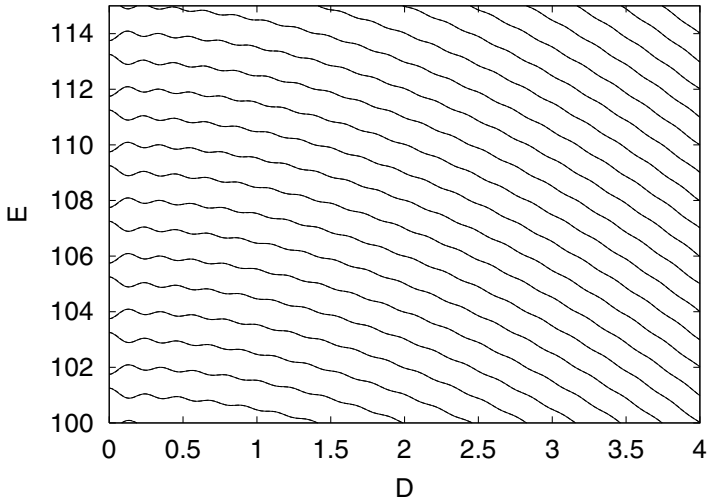

Figure 7. Comparison of the eigenvalues generated via the purely displacive transformation as a function of D with the numerically exact curves for $T = 0.25$ and $p = +1$. The two results are indiscernible on the scale of this figure.

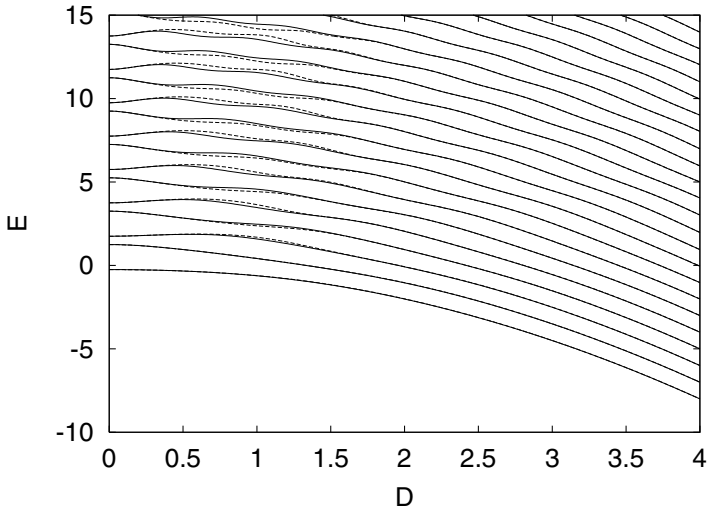

Figure 8. Comparison of the eigenvalues generated via the DA transformation as a function of D with the numerically exact curves for $T = 0.25$ and $p = +1$. Solid lines: exact numerical diagonalization, dashed lines: DA result.

that is optimal for higher states. Therefore the deviations in figure 8 are not a sign of a defect of the DA transformation itself, but are caused by an energetically non-optimal choice of the parameter values.

The results of the RD transformation show deviations which are somewhat larger than in the case of the DA transformation, (these are not shown here). Also the RD transformation contains the displacive transformation as a limit (for $\delta = D$, $\beta = 0$), so again an optimization of δ, β with respect to the ground state is no good overall optimization.

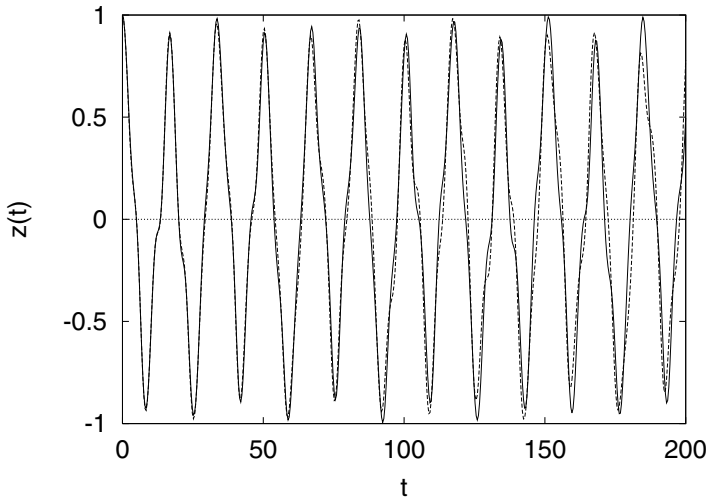

Figure 9. Occupation probability difference as a function of time. Comparison of the exact numerical solution (solid line) with the DA result (dashed line). Parameter values: coupling $D = 0.5$, transfer $T = 0.25$.

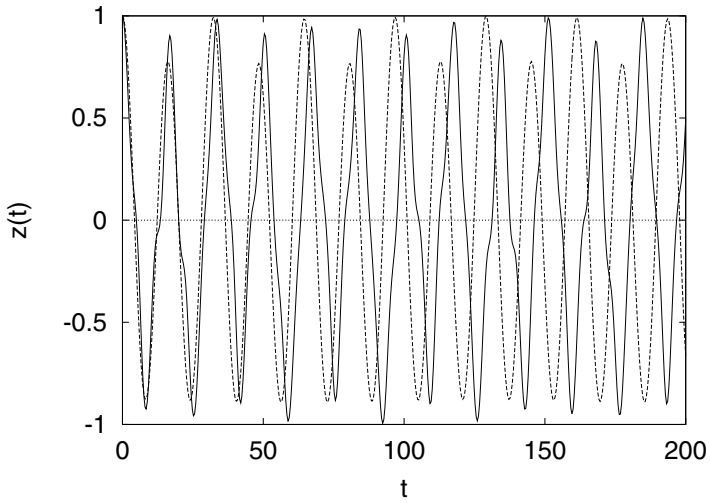

Figure 10. Occupation probability difference as a function of time. Comparison of the exact numerical solution (solid line) with the purely displacive result (dashed line). Parameter values: coupling $D = 0.5$, transfer $T = 0.25$.

6.1.2. Temporal evolution For $T = 0.25$ and $D = 0.5$ (weak coupling), the occupational difference $z(t)$ is shown for the DA transformation in figure 9, for the purely displacive transformation in figure 10, and for the semiclassical approximation in figure 11. In each case the approximated result is drawn with dashed lines, together with the numerically exact result, which is drawn with solid lines. The result of the RD transformation is omitted. It is very similar to the purely displacive one.

The most remarkable feature of these curves is that the DA evolution is considerably more accurate than the evolution of the purely displacive transformation (compare figures 9

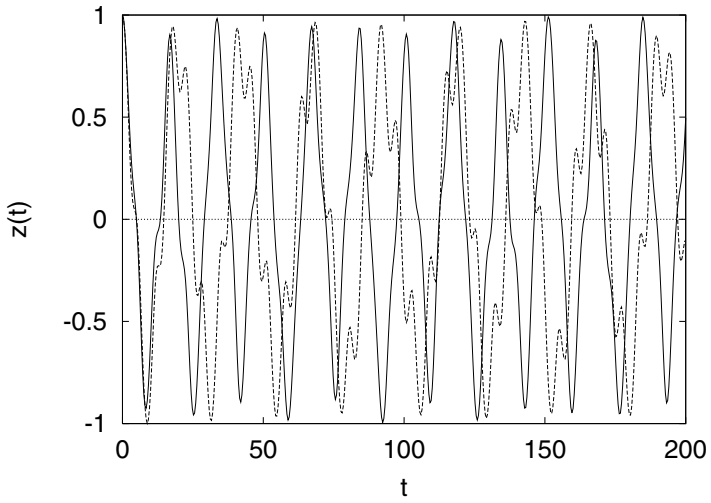

Figure 11. Occupation probability difference as a function of time. Comparison of the exact numerical solution (solid line) with the semiclassical result (dashed line). Parameter values: coupling $D = 0.5$, transfer $T = 0.25$.

and 10), although the latter is more accurate for the energy eigenvalues of the second and higher excited states (see figures 6 and 8). This is due to the fact that for small values of the coupling constant D, essentially only the lowest two eigenstates are occupied in each parity subspace. In particular, the main frequency of the oscillations of $z(t)$ is given by the difference between the two ground state energies $E_0^{(+)}$ and $E_0^{(-)}$. Since in our DA and RD transformations we optimize the transformational parameter to minimize the ground state energies, the latter are more accurate than in the case of the purely displacive transformation, where we have set $\delta = D$. In this parameter regime the improvement of the DA and RD transformations over the purely displacive one is therefore at least partly independent of the 'anticrossing' or 'reflective' component of the product transformations. However, to reproduce the analytically correct perturbation result a pure displacive transformation is not sufficient, as explained in the text following equations (36) and (43).

The semiclassical result (figure 11) is even more inaccurate than the displacive one.

For $T = 0.25$ and $D = 2$ (strong coupling), the evolution is presented in figure 12 for the DA transformation, in figure 13 for the purely displacive transformation, and in figure 14 for the semiclassical approximation. Again the RD result is omitted since it is almost identical to the displacive one. In this parameter regime the DA and the purely displacive transformation appear to capture different aspects of the exact result. While the displacive transformation correctly reproduces the overall behaviour of the exact curve, the internal short-time structure is completely missing. The DA transformation, on the other hand, is less accurate with respect to the overall behaviour, but is better in reproducing the short-time structures.

Finally it is seen that the semiclassical approximation is even qualitatively wrong for this combination of parameters.

6.2. Large transfer regime

6.2.1. Energy curves For the large transfer regime ($T = 2.5$) the D-dependency of the eigenenergies is shown

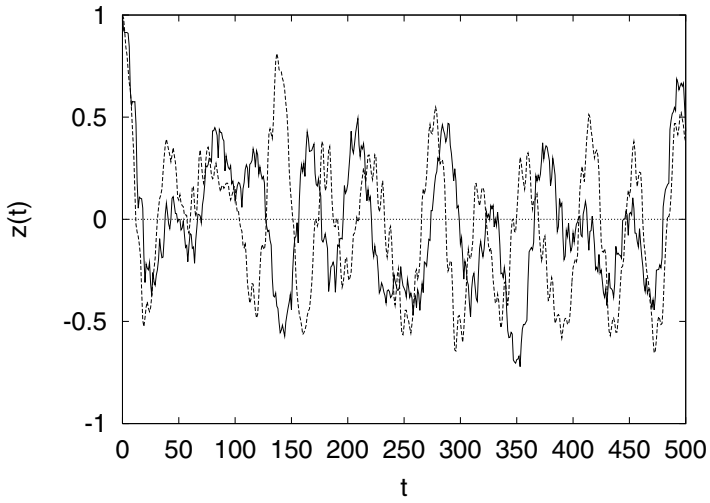

Figure 12. Occupation probability difference as a function of time. Comparison of the exact numerical solution (solid line) with the DA result (dashed line). Parameter values: coupling $D = 2$, transfer $T = 0.25$.

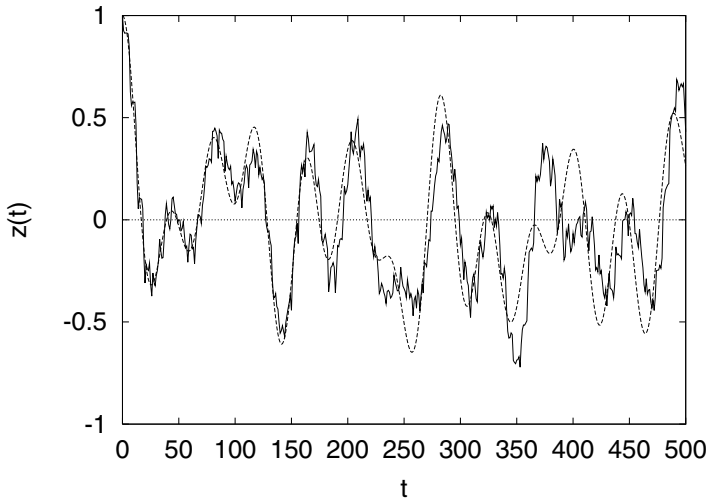

Figure 13. Occupation probability difference as a function of time. Comparison of the exact numerical solution (solid line) with the purely displacive result (dashed line). Parameter values: coupling $D = 2$, transfer $T = 0.25$.

- for the purely displacive transformation in figures 15 (low states, $n < 15$) and 16 (high states, $n \approx 100$),
- for the DA transformation in figures 17 (low states) and 18 (high states).

From the curves it can be seen that in the case of the low states for values of the coupling parameter up to $D \approx 1.5$ the DA results are significantly more accurate than the purely displacive ones, whereas for larger values of D both transformations have approximately the same accuracy. In the case of the high states the situation is different: For $D < 0.5$ the DA transformation is again decisively better than the displacive one, but for $0.5 < D < 2.5$ it

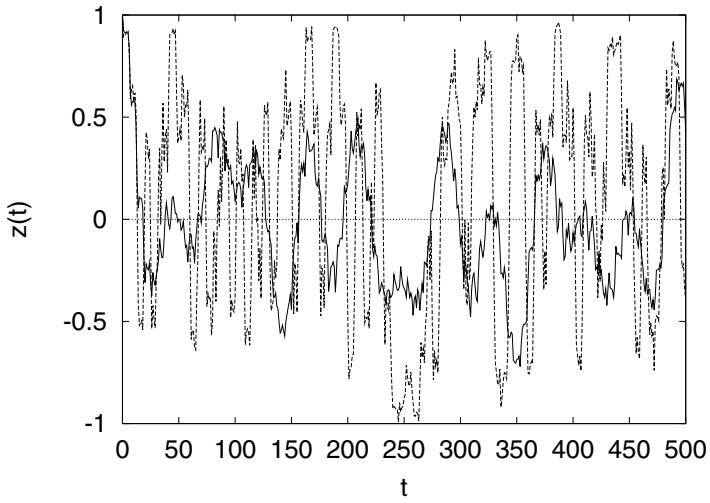

Figure 14. Occupation probability difference as a function of time. Comparison of the exact numerical solution (solid line) with the semiclassical result (dashed line). Parameter values: coupling $D = 2$, transfer $T = 0.25$.

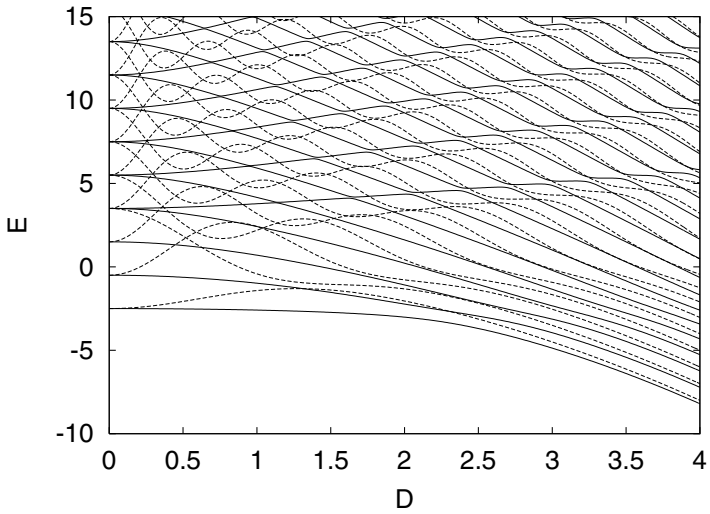

Figure 15. Comparison of the eigenvalues generated via the purely displacive transformation as a function of D with the numerically exact curves for $T = 2.5$ and $p = +1$. Solid lines: exact numerical diagonalization, dashed lines: purely displacive result.

is the purely displacive transformation which yields the better results. The reason for this behaviour is that the minimization of the ground states energy for the DA transformation leads to a discontinuity of the displacement parameter δ at $D \approx 2.5$, which is obvious from figures 17 and 18. In fact, for $D < 2.5$ δ is approximately equal to its analytical low-coupling value $\delta = D/(1 + 2T)$, and for $D > 2.5$ we have $\delta \approx D$.

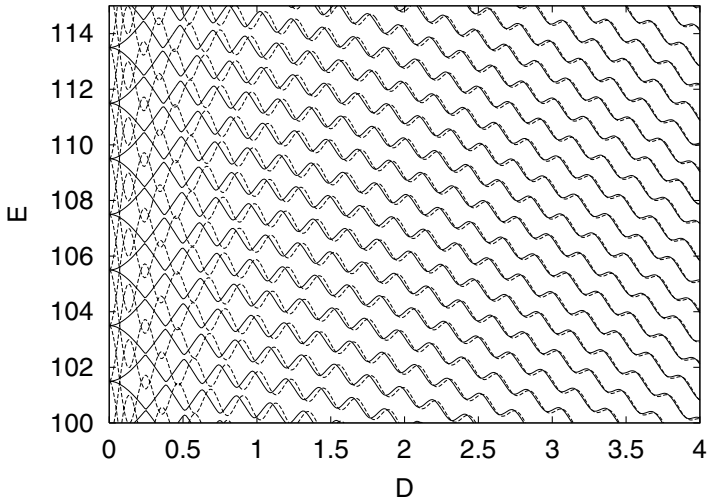

Figure 16. Comparison of the eigenvalues generated via the purely displacive transformation as a function of D with the numerically exact curves for $T = 2.5$ and $p = +1$. Solid lines: exact numerical diagonalization, dashed lines: purely displacive result.

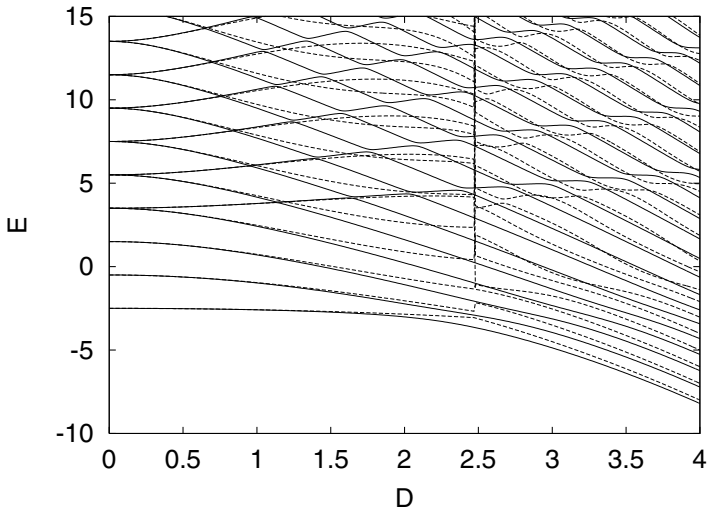

Figure 17. Comparison of the eigenvalues generated via the DA transformation as a function of D with the numerically exact curves for $T = 2.5$ and $p = +1$. Solid lines: exact numerical diagonalization, dashed lines: DA result.

To improve the results for the higher energy eigenvalues we move the δ discontinuity to $D = 0.5$, i.e., we regard δ as a given function of D of the form

$$\delta = \begin{cases} D/(1+2T) & \text{for } D < 0.5 \\ D & \text{for } D \geqslant 0.5 \end{cases} . \tag{80}$$

The results of this modified displacive-anticrossing (MDA) transformation are shown in figure 19 (for the low states) and figure 20 (for the high states). For the high states we now have a good agreement between the approximate and the exact energy values. However, for

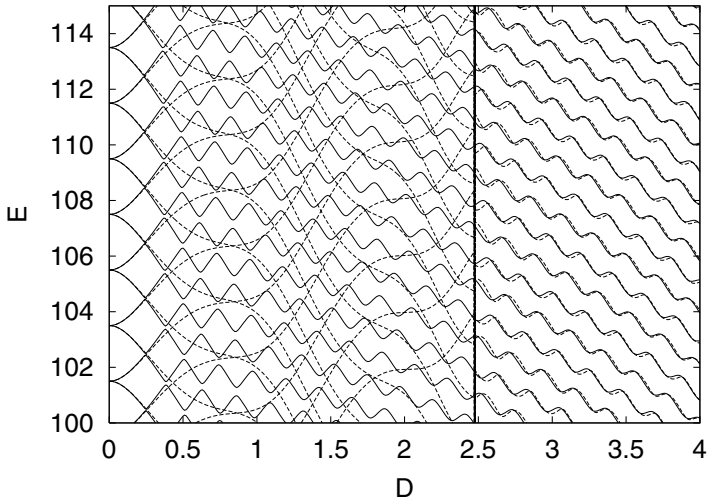

Figure 18. Comparison of the eigenvalues generated via the DA transformation as a function of D with the numerically exact curves for $T = 2.5$ and $p = +1$. Solid lines: exact numerical diagonalization, dashed lines: DA result.

the low energy states in the region $0.5 \leqslant D \leqslant 2.5$ the accuracy is now lower than in the case of the original DA transformation, although the results are at least as good as for the displacive transformation.

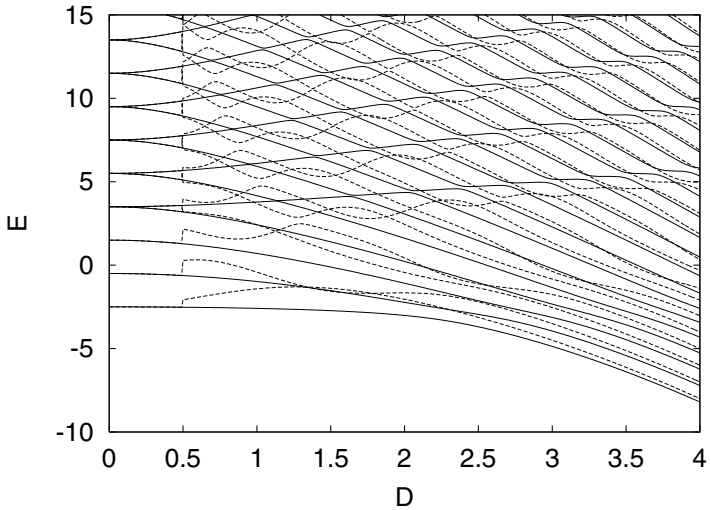

Figure 19. Comparison of the eigenvalues generated via the modified DA transformation as a function of D with the numerically exact curves for $T = 2.5$ and $p = +1$. Solid lines: exact numerical diagonalization, dashed lines: modified DA result.

We should take note here of an important flexibility of the DA transformation with respect to the choice of the parameter δ. If it happens that a specific fixed T–D-value combination makes the original DA choice for δ unsuitable, say for $D = 1$, $T = 2.5$, we may switch to another δ choice, such that the DA generation of the eigenbase is again good.

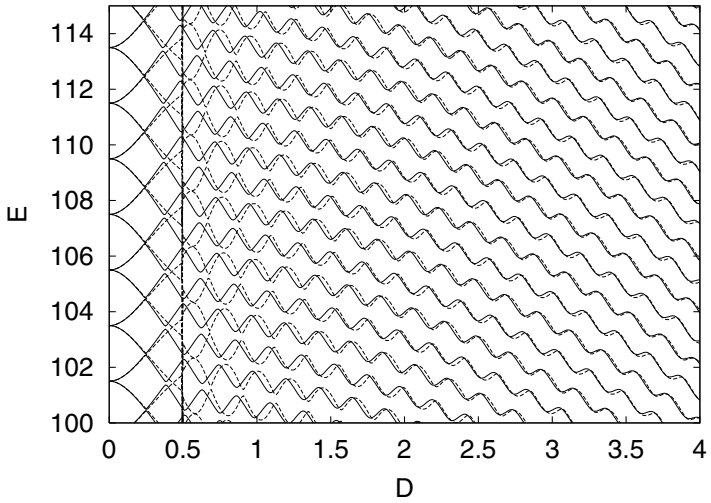

Figure 20. Comparison of the eigenvalues generated via the modified DA transformation as a function of D with the numerically exact curves for $T = 2.5$ and $p = +1$. Solid lines: exact numerical diagonalization, dashed lines: modified DA result.

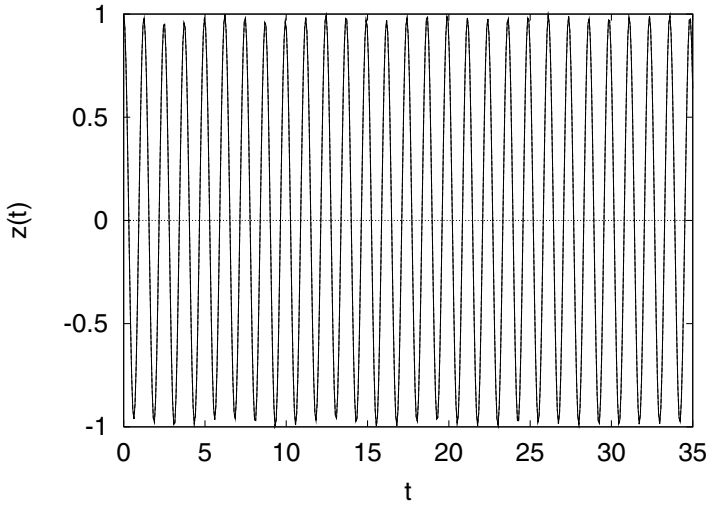

Figure 21. Occupation probability difference as a function of time. Comparison of the exact numerical solution with the DA result. The two results are indiscernible on the scale of this figure. Parameter values: coupling $D = 0.5$, transfer $T = 2.5$.

The RD result is omitted since it shows larger deviations from the exact result than the DA or the purely displacive transformations.

6.2.2. Temporal evolution For $T = 2.5$ and $D = 0.5$ (weak coupling) the result for the occupational difference $z(t)$ is shown in figure 21 for the DA transformation, in figure 22 for the displacive transformation and in figure 23 for the semiclassical approximation. Here the DA result is quantitatively correct; there is no visible difference between the DA and the exact curves. The same is true for the RD transformation, which is therefore not shown here. On the

other hand, the purely displacive transformation yields large deviations from the exact result, even larger than in the case of the semiclassical approximation. In this parameter regime the simple displacive transformation often used in the literature (see e.g. Steib *et al* [19]) clearly cannot reproduce the correct result, neither for the energy values nor for the temporal evolution.

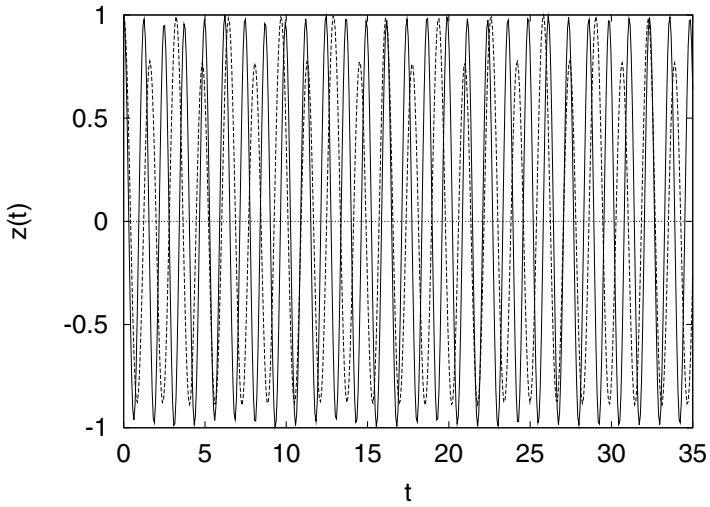

Figure 22. Occupation probability difference as a function of time. Comparison of the exact numerical solution (solid line) with the purely displacive result (dashed line). Parameter values: coupling $D = 0.5$, transfer $T = 2.5$.

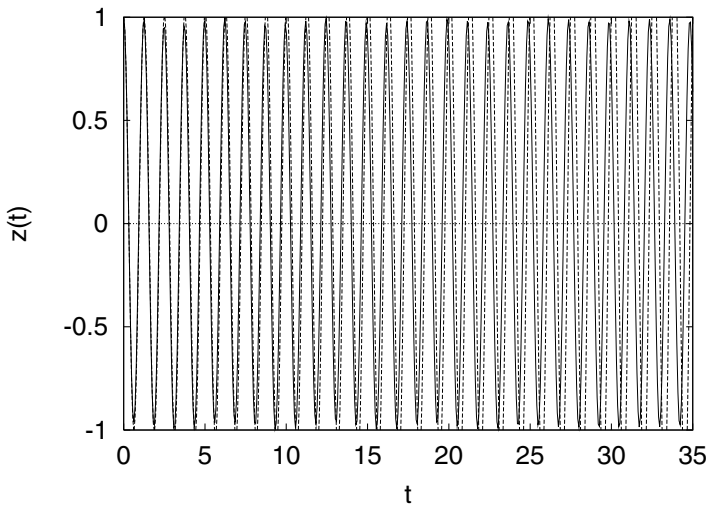

Figure 23. Occupation probability difference as a function of time. Comparison of the exact numerical solution (solid line) with the semiclassical result (dashed line). Parameter values: coupling $D = 0.5$, transfer $T = 2.5$.

For $T = 2.5$ and $D = 2$ (strong coupling), the DA result (figure 24) approximately reproduces the correct base frequency of the oscillations of $z(t)$, although the fluctuations of the amplitude are inaccurate. For the purely displacive transformation (figure 25), on the

other hand, the result is not only worse, but even qualitatively wrong. The semiclassical approximation (figure 26), on the other hand, shows the correct frequency, but the amplitude fluctuations are completely absent. Finally the RD result (figure 27) is better than the purely displacive one, but not as good as the DA result. Thus, in the large transfer and strong coupling regime only the DA transformation leads to a result which is semiquantitatively correct.

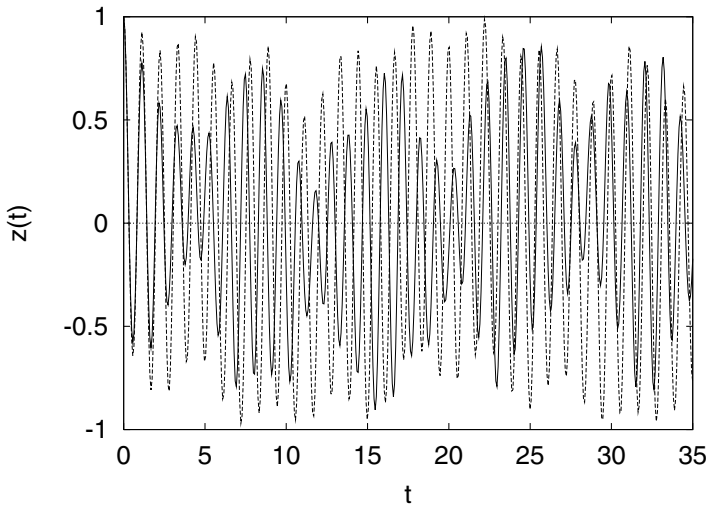

Figure 24. Occupation probability difference as a function of time. Comparison of the exact numerical solution (solid line) with the DA result (dashed line). Parameter values: coupling $D = 2$, transfer $T = 2.5$.

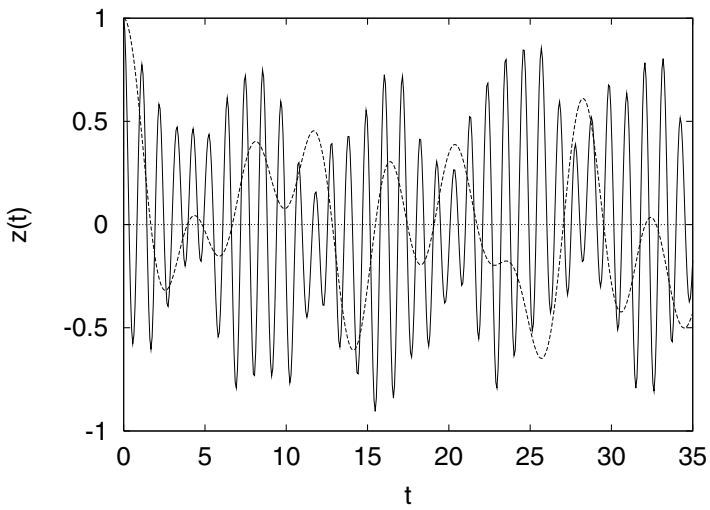

Figure 25. Occupation probability difference as a function of time. Comparison of the exact numerical solution (solid line) with the purely displacive result (dashed line). Parameter values: coupling $D = 2$, transfer $T = 2.5$.

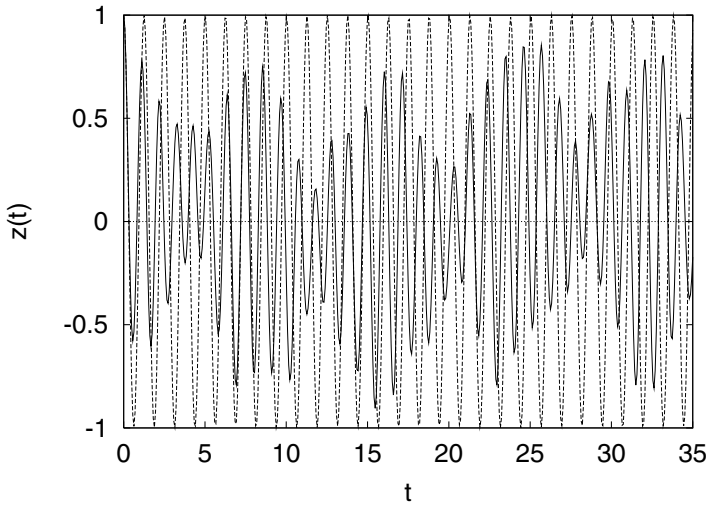

Figure 26. Occupation probability difference as a function of time. Comparison of the exact numerical solution (solid line) with the semiclassical result (dashed line). Parameter values: coupling $D = 2$, transfer $T = 2.5$.

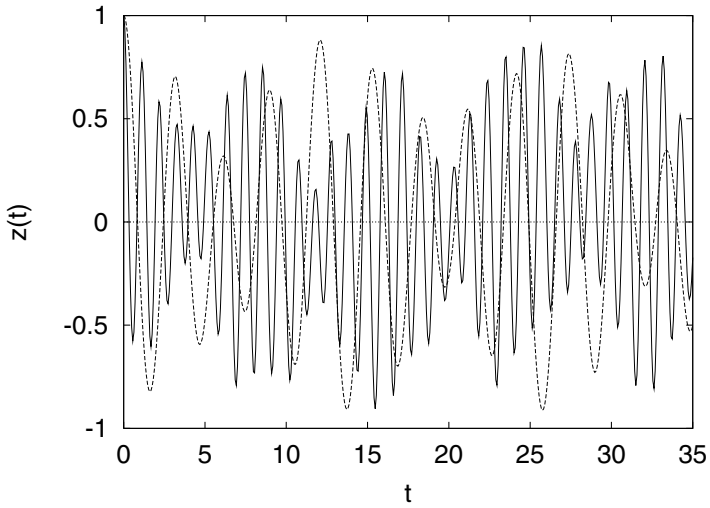

Figure 27. Occupation probability difference as a function of time. Comparison of the exact numerical solution (solid line) with the RD result (dashed line). Parameter values: coupling $D = 2$, transfer $T = 2.5$.

7. Conclusions and perspectives

We have presented a new method for investigating the temporal evolution of coupled excitonic-oscillatory systems, which is based on unitary transformations. In this method the two antagonistic tendencies of the coupled system (excitonic transfer versus polaronic localization) are handled by a unitary transformation of product form, in which each constituent accounts for one of the two tendencies.

Specifically we have considered two products of unitary operators, one of which being

of RD type and the other of DA type. In both cases we respectively have chosen the unitary operator factor of the most simple type, i.e. of a one parameter type. The parameters of the transformation have been optionally fixed by requiring an optimal diagonalization in the energetic sense. We have also indicated the possibilities of other parameter choices. The concept is such that the complete sequence of eigenvalues and eigenvectors of the Hamiltonian can be simultaneously generated by a transformation depending on only two parameters, without requiring an exact numerical diagonalization of the Hamiltonian.

The RD and the DA transformations already in their most simple forms have the virtue of yielding exact analytic diagonalization in the two opposing limits ($D \to 0$, T arbitrary and $T \to 0$, D arbitrary, where T, D respectively denote the transfer and coupling parameters of the Hamiltonian). In the former limit they satisfy the Fröhlich condition and are therefore equivalent to second-order perturbation theory.

In particular both our RD and our DA transformation reproduce correctly the 'Debye–Waller peculiarity' inherent in all exciton(electron)–phonon systems. This 'peculiarity' denotes the phenomenon that by means of the exciton–phonon coupling all odd power terms in the transfer parameter T are exponentially screened ('Debye–Waller screening') whereas the even power terms are not. This virtue renders the RD and DA transformations superior to other product transformations, such as e.g. a transformation of displacive-antisqueezing type, which frequently has been employed. Naturally our transformations are also superior to the purely displacive transformation, which is a limiting case of both our transformations, and which frequently has been used in the literature.

For comparison with exact results and with the semiclassical approximation we have applied our method to an archetypal two-site system, which can be also solved by numerical diagonalization. As expected from a perturbative analysis, the best results were obtained in the two opposite limiting cases $T \to 0$ and $T \to \infty$ (for fixed D) or in the two opposing limits $D \to 0$ and $D \to \infty$ (for fixed T).

Regarding the reproduction of the full eigenvalue spectrum, the DA transformation turns out to be best, yielding a semiquantitative reproduction in practically the full T–D-plane. There may, however, be certain T–D-values for which an applied optimization procedure of the transformation parameters (δ, α) is unsuitable. In these cases δ and α have to be chosen in a more suitable way.

Another outcome of our analysis is the critical evaluation of a Lang–Firsov type of transformation, which in our Fulton–Gouterman transcription of the Hamiltonian amounts to a purely displacive transformation (in oscillatory space). This type of transformation is the one most frequently used in earlier literature. It turns out that this transformation is only suitable for small transfer parameters T, whereas in other T–D regimes it may even be qualitatively wrong, or be even worse than the semiclassical approximation.

The semiclassical approximation, on the other hand, fails even qualitatively in regions of small T, and remains less accurate than the RD and DA results for larger T. In particular the symmetry-breaking behaviour that appears in the semiclassical approximation for small T and D, in contradiction to the exact result, is absent in the unitary transformation calculations.

Finally, we turn to the quality of our RD transformation. This transformation turns out to be almost as good as the DA transformation. Its shortcoming is revealed mainly in the energetic reproduction and it consists in its incapacity to inhibit the crossing of energy lines the latter for instance are discussed as functions of the Hamiltonian parameters (T or D). This results in a divergent behaviour for some critical T or D value ($T = T_c$ or $D = D_c$). However, if such a situation appears, one has the possibility of changing the choice of the transformation parameters such that the divergency is shifted to another location in the T–D-plane. It is therefore why the RD transformation is a good candidate for the generation of the eigenbase

of the Hamiltonian for any given values of T and D. We emphasize this, since it is the RD transformation which delivers the key for the generalization of our method (see below).

The aim of the present work has been to test the usability of the unitary transformation method for the 'dimer–oscillator' model. The next step would be to apply it to more complicated systems like extended, translationally invariant exciton–phonon systems, for which a numerically exact solution is not possible. Since the Fulton–Gouterman transformation can be generalized to such systems [31], a transformation similar to the RD one used in this paper may be employed to generate the approximate eigenstates of the Hamiltonian. In the case of a one-dimensional exciton–phonon chain the exponent S_r (equation (26)) of the reflective factor has to be replaced by an operator of translational type:

$$S_t^{(k)} = u_1^{(k)}(P_q, Q_q)R_1 + u_{-1}^{(k)}(P_q, Q_q)R_{-1} \tag{81}$$

where k denotes the wavevector of the total eigenfunction, $\{P_q, Q_q\}$ the phonon variables and $R_{\pm 1}$ a translational operator with the property $R_{\pm 1}Q_q = \mathrm{e}^{\pm \mathrm{i}q}Q_q R_{\pm 1}$. (For the Cartesian phonon coordinates,

$$Q_m = (N+1)^{-1/2}\sum_q \mathrm{e}^{\mathrm{i}qm}Q_q \tag{82}$$

we correspondingly have the rule $R_{\pm 1}Q_m = Q_{m\pm 1}R_{\pm 1}$.) The functional forms $u_{\pm 1}^{(k)}(P_q, Q_q)$ must be chosen in a suitable manner.

Appendix: The displacive-antisqueezing transformation

In this appendix we consider an alternative transformation, composed of a displacive transformation and an antisqueezing transformation:

$$U = U_a(\alpha)U_d(\delta) = \exp\bigl(-\mathrm{i}\alpha(PQ + QP)\bigr)\exp(\mathrm{i}\delta P). \tag{A.1}$$

This transformation has previously been applied to the dimer model by Sonnek *et al* [20], who found that it yields acceptable results for the ground state in the weak-coupling regime only. Here we will discuss on the one hand, whether these result can be carried over to excited states, and on the other, whether the transformation is analytically appropriate for the weak transfer case ($T \ll 1$, D arbitrary) also.

The transformed Hamiltonian reads

$$\tilde{H}_{\mathrm{FG}}^{(p)} = U^{\dagger}H_{\mathrm{FG}}^{(p)}U = \tfrac{1}{2}[\mathrm{e}^{-4\alpha}P^2 + \mathrm{e}^{4\alpha}(Q-\delta)^2] + \mathrm{e}^{2\alpha}D(Q-\delta) - pTR_Q\mathrm{e}^{2\mathrm{i}\delta P} \tag{A.2}$$

and the energy expectation value in the ground state is

$$E_0^{(p)} = \tfrac{1}{2}[\delta^2\mathrm{e}^{4\alpha} + \cosh(4\alpha)] - D\delta\mathrm{e}^{2\alpha} - pT\mathrm{e}^{-\delta^2}. \tag{A.3}$$

Appendix A.1. Weak coupling regime

As we will see later, in the weak coupling regime ($D \ll 1$) δ is of order D and α of order D^2. Therefore we expand $\tilde{H}_{\mathrm{FG}}^{(p)}$ up to terms quadratic in δ and linear in α:

$$\begin{aligned}\tilde{H}_{\mathrm{FG}}^{(p)} = {} & \tfrac{1}{2}(P^2+Q^2) - pTR_Q + (D-\delta)Q + 2\mathrm{i}pT\delta PR_Q + 2\alpha(Q^2-P^2) \\ & -D\delta + \tfrac{1}{2}\delta^2 + 2pT\delta^2P^2R_Q + O(\delta^3, \alpha\delta, \alpha^2).\end{aligned} \tag{A.4}$$

Applying $\tilde{H}_{\mathrm{FG}}^{(p)}$ to the ground state $|\phi_0^{(0)}\rangle$ yields

$$\begin{aligned}\tilde{H}_{\mathrm{FG}}^{(p)} = {} & \bigl(\tfrac{1}{2} + pT(1-\delta^2)\bigr)|\phi_0^{(0)}\rangle + \frac{1}{\sqrt{2}}[D - (1+2pT)\delta]|\phi_1^{(0)}\rangle \\ & +\sqrt{2}(2\alpha - pT\delta^2)|\phi_2^{(0)}\rangle + O(\delta^3, \alpha\delta, \alpha^2).\end{aligned} \tag{A.5}$$

Setting $\delta = D/(1+2pT)$, $\alpha = \frac{1}{2}pT\delta^2$ makes $|\phi_0^{(0)}\rangle$ an eigenvector of $\tilde{H}_{\mathrm{FG}}^{(p)}$ up to $O(D^2)$. However, when the same Hamiltonian is applied to state $|\phi_1^{(0)}\rangle$, there appear non-diagonal terms of order D. So the displacive-antisqueezing transformation can diagonalize the Hamiltonian only for the ground state of the system. This is in contrast to the RD and the DA transformations, which in the weak coupling regime fulfill the Fröhlich condition and therefore diagonalize the Hamiltonian for all states (see subsection 3.1.3).

Appendix A.2. Weak transfer regime

In the case of vanishing transfer ($T = 0$), exact diagonalization is obtained for $\delta = D$, $\alpha = 0$. Therefore we set $\delta = D + \delta'$ and expand $E_0^{(p)}$ up to quadratic terms in α and δ':

$$E_0^{(p)} = \tfrac{1}{2} - \tfrac{1}{2}D^2 - pT\mathrm{e}^{-D^2} + 2pTD\mathrm{e}^{-D^2}\delta' + \left(\tfrac{1}{2} - pT(2D^2-1)\mathrm{e}^{-D^2}\right)\delta'^2 + 2D\alpha\delta' + 2(D^2+1)\alpha^2. \tag{A.6}$$

The minimal value of $E_0^{(p)}$ is obtained for

$$\alpha = \frac{pTD^2\mathrm{e}^{-D^2}}{1 - 2pT(2D^2-1)(D^2+1)\mathrm{e}^{-D^2}} \tag{A.7}$$

$$\delta' = -\frac{2pTD\mathrm{e}^{-D^2}}{1/(D^2+1) - 2pT(2D^2-1)\mathrm{e}^{-D^2}}. \tag{A.8}$$

If the coupling is strong ($D \gg 1$), terms containing the Debye–Waller factor e^{-D^2} can be neglected compared to algebraic terms, and we obtain

$$\alpha = pTD^2\mathrm{e}^{-D^2} \tag{A.9}$$

$$\delta' = -2pTD(D^2+1)\mathrm{e}^{-D^2} \tag{A.10}$$

$$E_0^{(p)} = \tfrac{1}{2} - \tfrac{1}{2}D^2 - \mathrm{e}^{-D^2}pT + 2D^2(1-D^2)\mathrm{e}^{-2D^2}T^2 + O(T^3). \tag{A.11}$$

Thus the displacive-antisqueezing transformation yields an even stronger Debye–Waller screening in the T^2 term of the ground state energy. However, as we have stated in section 5, the correct analytic behaviour should not contain a Debye–Waller screening $\exp(-D^2)$ in the even power terms of T (Debye–Waller peculiarity). Thus the displacive-antisqueezing transformation is unable to reproduce the correct analytic result.

References

[1] Landau L D 1933 *Phys. Z. Sowjetunion* **3** 664
[2] Alexandrov A S and Mott N F 1994 *Rep. Prog. Phys.* **57** 1197
[3] Ranninger J 1991 *Z. Phys.* B **84** 167
[4] Mott N F 1973 *Cooperative Phenomena* ed H Haken and M Wagner (Berlin: Springer) p 2
[5] Mott N F 1995 *Polarons and Bipolarons in High-T_c Superconductors and Related Materials* ed E K H Salje, A S Alexandrov and W Y Liang (Cambridge: Cambridge University Press) chap 1
[6] Alexandrov A and Ranninger J 1981 *Phys. Rev.* B **23** 1796
Alexandrov A and Ranninger J 1981 *Phys. Rev.* B **24** 1164
[7] Schafroth M R 1955 *Phys. Rev.* **100** 463
[8] Hu X and Schulten K 1997 *Phys. Today* **50** 28
[9] Barvík I, Warns Ch, Neidlinger Th and Reineker P 1999 *Chem. Phys.* **240** 173
[10] Fugol' I Ya 1988 *Adv. Phys.* **37** 1
[11] Lushchik Ch B 1982 *Excitons* ed E I Rashba and M D Sturge (Amsterdam: North-Holland) p 505
[12] Kenkre V M and Wu H-L 1989 *Phys. Rev.* B **39** 6907
[13] Esser B and Schanz H 1995 *Z. Phys.* B **96** 553

[14] Herfort U and Wagner M 1997 *Phys. Rev.* B **56** 8702
[15] Herfort U and Wagner M 1999 *Phil. Mag.* B **79** 1931
[16] Herfort U and Wagner M 2000 *J. Mol. Liquids* **86** 91
[17] Wagner M 1986 *Unitary Transformations in Solid State Physics* (Amsterdam: North Holland)
[18] Silbey R and Harris R A 1984 *J. Chem. Phys.* **80** 21625
[19] Steib R, Schoendorff J L, Korsch H J and Reineker P 1998 *Phys. Rev.* E **57** 6534
[20] Sonnek M, Frank Th and Wagner M 1994 *Phys. Rev.* B **49** 15637
[21] Holstein T 1959 *Ann. Phys., NY* **8** 325
[22] Shore H B and Sander L M 1973 *Phys. Rev.* B **7** 4537
[23] Wagner M and Köngeter A 1990 *J. Lumin.* **45** 235
[24] Sonnek M, Eiermann H and Wagner M 1995 *Phys. Rev.* B **51** 905
[25] Rapp M 1999 *PhD Thesis* University of Stuttgart
[26] Wagner M 1985 *J. Phys. A: Math. Gen.* **18** 1915
[27] Gradshteyn I S and Ryzhik I M 1994 *Table of Integrals, Series and Products* 5th edn (New York: Academic)
[28] Kenkre V M and Campbell D K 1986 *Phys. Rev.* B **34** 4959
[29] Firsov Y A and Kadinov E K 1997 *Phys. Solid State* **39** 1930
[30] Firsov Y A, Kabanov V V, Kudnikov E K and Alexandrov A S 1999 *Phys. Rev.* B **59** 12132
[31] Wagner M 1984 *J. Phys. A: Math. Gen.* **17** 2319